Journal of Bionic Engineering
https://doi.org/10.1007/s42235-022-00226-9

RESEARCH ARTICLE

Human-Exoskeleton Joint Coordination Assessment: A Case Study on the Shoulder and Elbow Joints

Pablo Delgado[1] · **Clarissa Rincon**[2] · **Yimesker Yihun**[1]

Received: 29 March 2022 / Revised: 23 May 2022 / Accepted: 24 May 2022

Abstract
This study is aimed at developing a methodology to assess and quantify the human limb motions and interactions with the exoskeleton in relation to alignment. Three different basic and common upper arm joint movements and their interaction with a joint-based exoskeleton are considered: shoulder vertical and horizontal abduction–adduction, and elbow flexion–extension. The exoskeleton and the human model are aligned to the respective joints inside a Musculoskeletal Modeling software. Within the range of motion, the linear and angular displacement errors were analyzed, and the effect of those errors on the length of the associated tendons was studied. Results have shown a noticeable variation of the muscle-tendon lengths up to 65.7 mm and a change in the pattern on different muscle groups of the shoulder. Similarly, about 4 mm muscle-tendon length changes observed particularly at the elbow anconeus muscle-tendon. These changes of length could cause unwanted stresses at the joints, specially for people with disabilities due to stroke that might not have the flexibility to accommodate those extra pose variations imposed by the exoskeleton.

Keywords Exoskeleton · Upper limb · Rehabilitation · Misalignment · OpenSim · Computational modeling · Bioinspiration

1 Introduction

The need for robotic systems in human rehabilitation arose when medical and rehabilitation research areas began to search for an alternative rehabilitation method that could induce active involvement from the patient through an active system, which would lead to a more effective and rapid recovery [1]. This new method that incorporated the robotic devices began to provide benefits to the rehabilitation process by reducing the physical load upon the physical therapist, allowing longer training periods, reducing muscle strain upon the patient, and reducing localized muscle activity within the patient's targeted limb [2–4]. Therefore, rehabilitation and ergonomic areas have continued to motivate involvement in exoskeleton research over the years.

As new exoskeleton designs are proposed, there exists the need for their assessment and evaluation to ensure user safety and effectiveness. The quantitative evaluation of the kinematic compatibility between the human body and an exoskeleton is a crucial measure in the assessment process since there is a relative motion from human-exoskeleton interactions that could lead to negative effects upon the user [5]. Moreover, a common challenge in exoskeleton development arises when it comes to the alignment of these robotic devices to the anatomical structure of the human body [6]. These misalignment issues are prevalent in exoskeleton designs that have a focus on mimicking and simplifying the human body due to the complexity of the human joints. Typically, complex joints, such as the shoulder and elbow joints, are modeled as ball-and-socket and hinges joints respectively. However, this design approach creates a limited range of motion, which causes inconsistency between the human limb's trajectory and that of the exoskeleton [7]. In addition, it creates the assumption that the set of joints has a fixed frame that represents the joint position and/or rotation when in fact, certain sets of joints allow for complex motions that result in displacement of its center of rotation [6]. Therefore,

✉ Yimesker Yihun
yimesker.yihun@wichita.edu

Pablo Delgado
padelgado@shockers.wichita.edu

Clarissa Rincon
cxrincon@shockers.wichita.edu

[1] Mechanical Engineering, Wichita State University, 1845 Fairmount, Wichita, KS 67260, USA

[2] Biomedical Engineering, Wichita State University, 1845 Fairmount, Wichita, KS 67260, USA

Published online: 14 July 2022

failure to align these robotic devices to the anatomical structure of the human body can cause constraints and stress upon the targeted limbs and joints as well as affect the user's agility of movement [8–10]. Furthermore, there have been several attempts on solving this recurring issue of misalignment within exoskeleton designs, however, most solutions do not take into account all of the different segments of the human body's range of motion and how the motion differs among individuals.

Overall, joints are one of the most sensitive parts of the human body, and they are significantly difficult to investigate as their rotational axis is constantly changing within the clearance of the joint throughout every single task. A realistic characterization of the process that accounts for a changing geometry of the joints as well as contact interfaces is required. Human joints have been modeled based on kinematics, bone contact, muscle, and ligament force interactions through prototype testing and computational modeling and simulation [11, 12]. For instance, the study shown in [13] provides an analytical and experimental analysis on an upper limb exoskeleton design through prototype testing. By studying the supported range of motion experimentally, they were able to determine a compatibility between the designed exoskeleton's range of motion and the natural range of motion of the human arm. In addition, certain studies aim to assess exoskeletons on their ability to account for human variability and alignment to the human body. For instance, a study introduces a model-based assessment method that involves simulation to assess the kinematics of an exoskeleton by identifying the source of parasite forces at the attachment points between the exoskeleton and the human subject in the prototyping stage [14].This approach does not estimate the magnitude of those forces, which cannot then quantify the level of impairment nor the parasite forces at the joints. Similarly in [15], the OpenSim software is used to predict the dynamic behavior of a human-exoskeleton system, however, the effects of this interaction on the human muscles and potential consequences are not presented. In another study, [16] the OpenSim software has been utilized to aid the exoskeleton development process by allowing the observation of the kinematics of a desired motion in the human-exoskeleton interaction, however,there has not been an overall focus on using the software as a means to quantify the misalignment of an exoskeleton and its effects on the targeted limb. In [17], a 3D relative motion exoskeleton assessment method using a motion capture system is presented. In this method, the kinematic information of a human-exoskeleton system is extracted from reflective markers and the relative orientation between the human joint and exoskeleton joint is compared. However, information regarding the relative displacement is not presented, limiting its usefulness for joints that suffers translation during its range of motion, i.e. the shoulder joint [18]. Furthermore, due to the nature of the exoskeleton, the relative position of the human joints can be already constrained, which may reflect the wrong position of the center of rotation of the human joint. The study in [19] introduces a method of detecting and quantifying undesired interaction forces caused by joint misalignment to validate a proposed fixation mechanism that is expected to decrease the magnitude of the forces. The assessment method involves human subject testing under virtual environments where the interaction forces were collected and compared using a six-axis force torque (F/T) sensor. Although the F/T sensor was successful at quantifying the undesired interaction forces caused by the joint misalignment, a method was not provided to quantify the misalignment itself. This method would also require a developed prototype of the designed exoskeleton. On other hand, if the exoskeleton were to be assessed virtually through modeling and simulation, a prototype would not need to be developed until proper alignment is ensured.

In this study, a methodology to assess and quantify the misalignment of a human-exoskeleton system at the design stage using the kinematic information of the exoskeleton and the OpenSim software is presented. The effects of misalignment is quantified by examining the changes in muscle tendons. The proposed approach will be presented in a case study on the shoulder and elbow joints using a joint-based exoskeleton for upper limb rehabilitation. Despite using this type of exoskeleton, our work can be easily applied to assess other types of exoskeletons, as well as target other parts of the human body. The novelty of our approach lies on the fact that the wearable exoskeleton can be assessed without compromising real subjects since it is conducted in a simulation environment, and the ability to directly evaluate and quantify the misalignment and its effects on the muscles.

The results obtained through this assessment can serve as guidance to exoskeleton designers and developers to improve their design toward the development of optimal exoskeletons by minimizing the joint impairments between the robotic devices and human joints. In effect, this will reduce unwanted constraints in muscle-tendon lengths which might cause severe pain to a patient undergoing rehabilitation. Furthermore, higher impairment should be expected in physical systems, since perfect alignment between an exoskeleton and the human body is a challenge to achieve due to the complexity of the determined physical frames within the joints since they are located under the skin, surrounded by muscles.

2 Exoskeleton Description

In this study, a prototype of a 4 Degrees-of-Freedom (DOF) upper limb joint-based exoskeleton (Fig. 1) and its interaction with human joints is studied. The main body of the exoskeleton is composed of four rigid bodies: link 1,

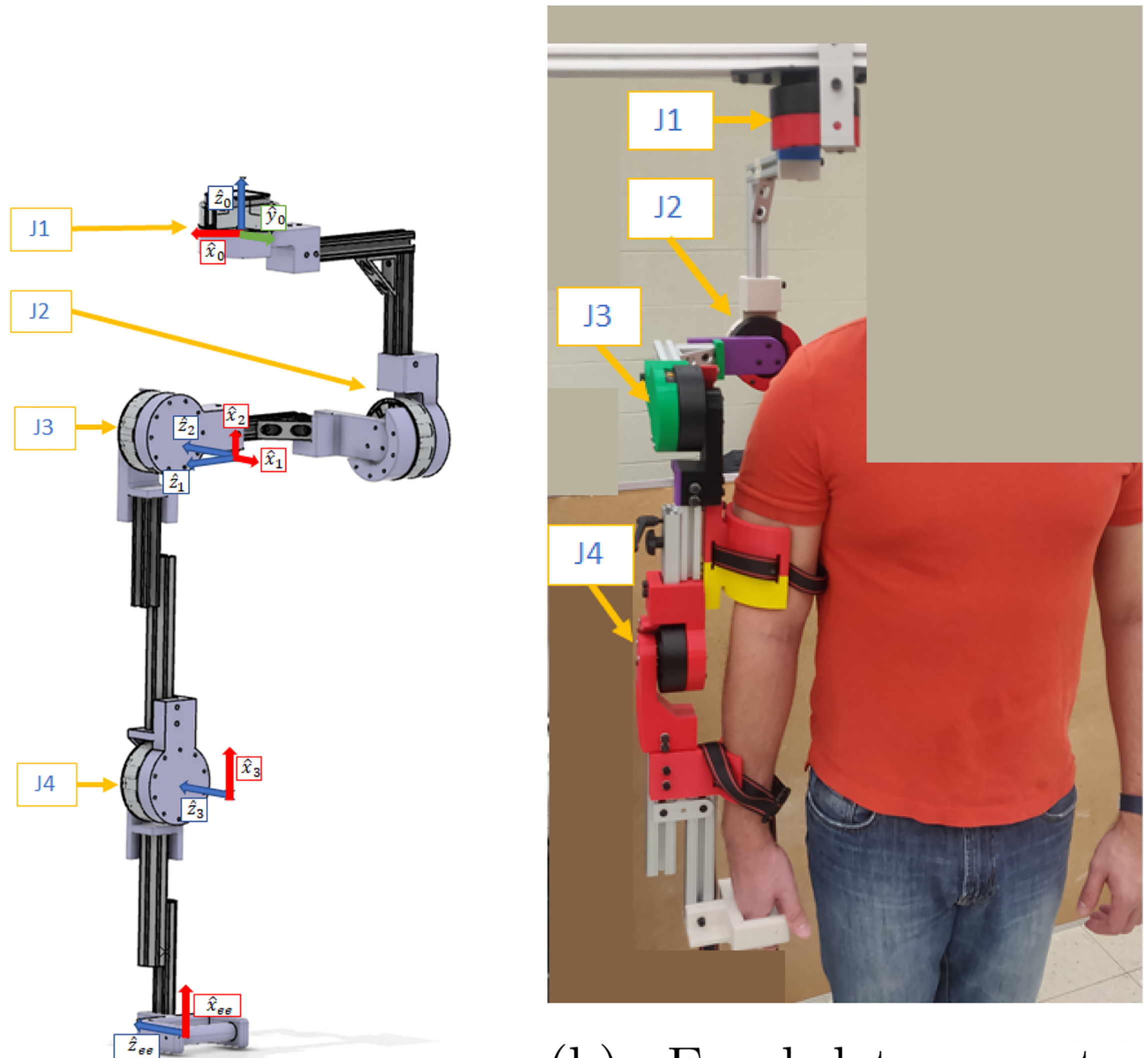

(a) CAD model

(b) Exoskeleton prototype

Fig. 1 Exoskeleton with four degrees-of-freedom

link 2, link 3, and link 4. These bodies are interconnected through mechanical revolute joints (J_1, J_2, J_3, and J_4), respectively. The shoulder joint is modeled as a 3-DOF ball-and-socket joint, with a center of rotation at the point where the axes of the joints J_1, J_2 and J_3 intercepts with one another. Each joint has a relative orientation of 90° with respect to each other's axis of rotation ($\hat{z}_1, \hat{z}_2$, and $\hat{z}_3$). Similarly, the elbow joint is modeled as a 1-DOF hinge type joint (J_4), with an axis of rotation labeled as $\hat{z}_4$. In addition to the active joints, this prototype has two additional passive-translational joints along link 3 and link 4 that allow proper adjustment of the exoskeleton arm to fit different anthropometric measurements of users.

3 OpenSim and Musculoskeletal Human Model

In this study, the free-software OpenSim is used to model and simulate the range of motion of the exoskeleton and the human model, given the generalized coordinates of their respective joints [20]. The software offers a series of tools to solve for Inverse Kinematics (IK) and Inverse Dynamics (ID), that determine the forces and torques at the joints required to generate the desired trajectories. The software also offers several approaches that extend the ID toolbox to solve for the net forces exerted by each muscle. Additionally, given the generalized coordinates of a motion obtained from the IK toolbox, OpenSim reports the changes on muscle tendons' length at each time step of the simulation. Our work will focus on the corresponding changes in muscle tendons' length due to joint impairment between the human model and the exoskeleton.

For the study, the Stanford VA Upper Limb Model is used as the human musculoskeletal model [21, 22], Fig.2. This model of the upper extremity is composed of 50 muscles that cross its 15 DOFs, representing the shoulder, elbow, forearm, and wrist. This human model does not use a spherical joint to mimic the kinematics of the human shoulder; instead, it simulates the actual human joint by modeling the sterno-clavicular rhythm. This means that the center of rotation of the shoulder joint does not remain fixed throughout the range of motion of the shoulder joint. Therefore, this model is suitable for the presented study, where the misalignment between a rigid-body robotic system and a human model is assessed and its effects are presented through simulation.

4 Human-Exoskeleton System Interaction: Case Study

In these cases of study, the misalignment and its potential effects between a joint-based exoskeleton and the human upper limb model are addressed through computational simulations. For this purpose, the exoskeleton model, the human model, and the software presented in the Sects. 2 and 3 are used. The human-exoskeleton system is presented in Fig. 3, where the alignment of each respective joint is highlighted. Both systems are scaled to the appropriate measurements, assuring that the center of rotation for the glenohumeral joint and the center of rotation of the exoskeleton are coincident at the beginning of the motion, Fig. 3a. The alignment was achieved by adding a 6-DOF joint for both systems at their respective bases, then moving and rotating them until the calibration was achieved. The axes of the frames representing the human model and the exoskeleton are $\{\hat{x}_{\text{hum}}, \hat{y}_{\text{hum}}, \hat{z}_{\text{hum}}\}$ and $\{\hat{x}_{\text{exo}}, \hat{y}_{\text{exo}}, \hat{z}_{\text{exo}}\}$, respectively. Fig. 3b shows the misalignment between the center of rotations at a position during shoulder flexion movement. Similarly, the axis of rotation of the elbow joint and of the J_4 exoskeleton joint must coincide with one another, Fig. 3c. However, as motion is induced on the elbow, the axes of rotation of the exoskeleton and model elbow joint are not coincident with each other, Fig. 3d. These adjustments must be made when all the joint parameters are set to 0°; in other words, when the human model arm and exoskeleton arm are parallel to the sagittal plane (parallel to the human body's Thorax).

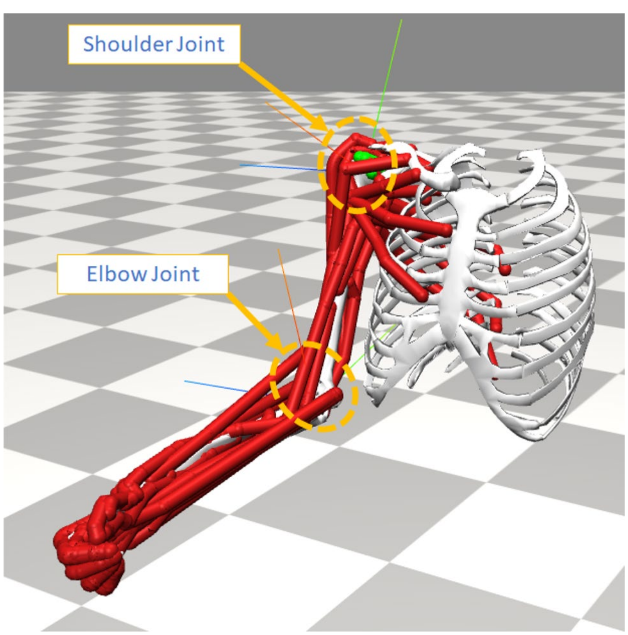

Fig. 2 Stanford VA Upper Limb Model

Once the exoskeleton system and human model are aligned, three different typical rehabilitation exercises are performed: shoulder abduction–adduction, shoulder flexion–extension, and elbow flexion–extension. The goal is to feed a set of generalized coordinates to the system that will then reproduce the desired tasks, with a range of motion from 0° to 130°, then from 130° to 0° for the duration of 4 seconds. Simulations from OpenSim yield files containing information about each system kinematics during the task at the Center of Mass (CoM) with respect to the ground frame, $\{s\}$, making the comparison between the relative positions (x, y, and z coordinates) and orientations (α, β, and γ Euler angles) of the bodies of interest possible. To make OpenSim report the actual position of the joints, virtual bodies with negligible masses and inertia tensors, and CoM at the joints were added. Theoretically, if there is proper alignment between the exoskeleton and the human model, the relative body transformation between the joints must remain constant.

For the analysis of the relative transformation between the bodies, a position offset and fixed rotation of the frame of interest is determined at $t = 0$. Hence, if the relative position and orientation is constant, then the corresponding errors will be equal to zero. The position error is presented in Eq. 1. This a necessary step, especially for the elbow joint since the location of the frames representing each transformation in the exoskeleton and human system might not lie on the same location.

$$\boldsymbol{e}_p(\boldsymbol{t}) = \boldsymbol{P}_{\text{exo}}(\boldsymbol{t}) - \boldsymbol{P}_{\text{hum}}(\boldsymbol{t}) - \boldsymbol{e}_p(\boldsymbol{0}) \tag{1}$$

where $\boldsymbol{e}_p(\boldsymbol{t})$ is the position error, $\boldsymbol{P}_{\text{exo}}(\boldsymbol{t}) = [x_{\text{exo}}(t), y_{\text{exo}}(t), z_{\text{exo}}(t)]^T$ is the position vector at the origin of the exoskeleton joint, and $\boldsymbol{P}_{\text{hum}}(\boldsymbol{t}) = [x_{\text{hum}}(t), y_{\text{hum}}(t), z_{\text{hum}}(t)]^T$ is the position vector at

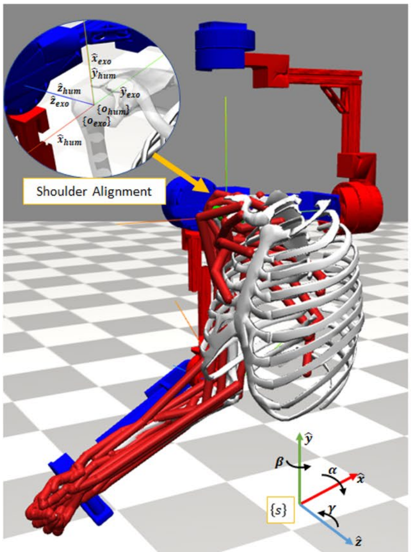

(a) Aligned shoulder-exoskeleton joints

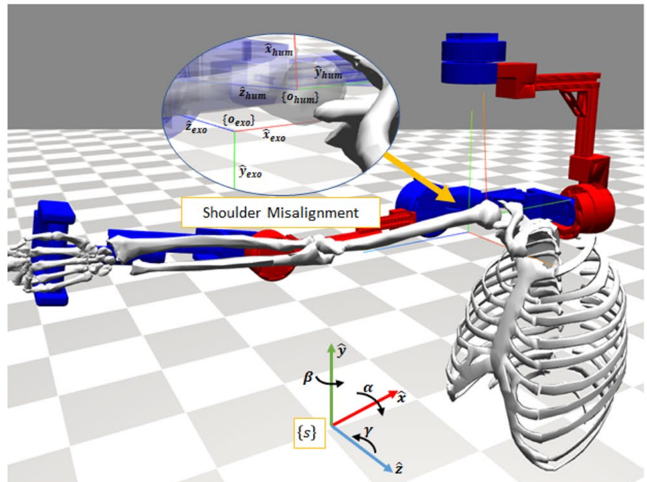

(b) Shoulder-exoskeleton alignment during flexion

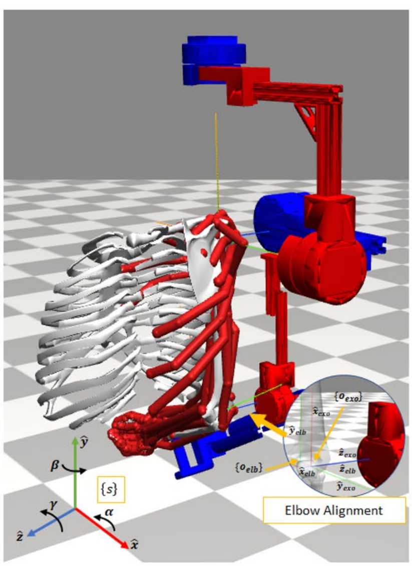

(c) Elbow-exoskeleton alignment

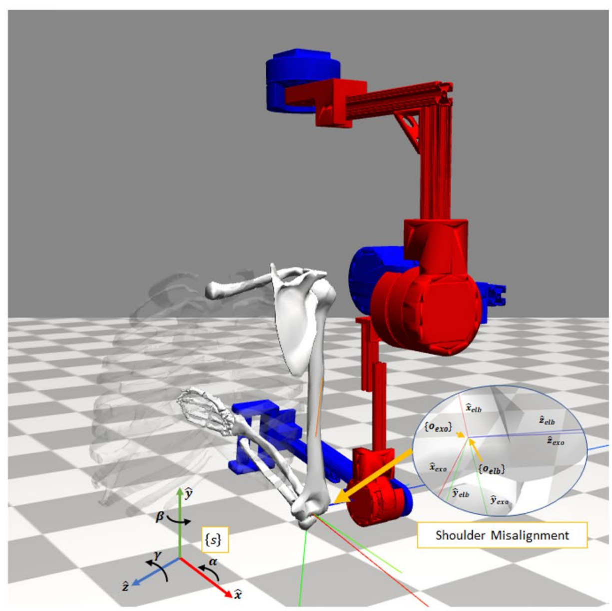

(d) Elbow-exoskeleton misalignment

Fig. 3 Musculoskeletal–exoskeleton system

the origin of the human model joint. Likewise, the error in the relative orientation is presented in Eq. 2.

$$\boldsymbol{e_q(t)} = \boldsymbol{Q}_{\text{exo}}\boldsymbol{(t)} - \boldsymbol{Q}_{\text{hum}}\boldsymbol{(t)} \tag{2}$$

where $\boldsymbol{e_q(t)}$ is the orientation error, $\boldsymbol{Q}_{\text{exo}}\boldsymbol{(t)} = [\alpha_{\text{exo}}(t), \beta_{\text{exo}}(t), \gamma_{\text{exo}}(t)]^T$ is the orientation vector representing the exoskeleton joint, and $\boldsymbol{Q}_{\text{hum}}\boldsymbol{(t)} = [\alpha_{\text{hum}}(t), \beta_{\text{hum}}(t), \gamma_{\text{hum}}(t)]^T$ is the orientation vector the human joint.

4.1 Shoulder Abduction–Adduction Task

For this task, the J_2 exoskeleton joint was actuated from 0° to 130° during 4 seconds. The other joints were locked at 0° during the entire trajectory. Then, the generalized coordinates of the human model were programmed to produce the shoulder abduction–adduction task while maintaining a synchronize range of motion with its robotic counterpart. The resultant position and orientation errors are presented in Fig. 4. The position error in $\hat{x}$ varies from − 40.34 mm to 0 mm, $\hat{y}$ varies from − 40.95 mm to 0 mm, and $\hat{z}$ varies from − 24.58 mm to 0 mm. Additionally, the orientation error in α varies from 0° to 0.22°, β varies from −5.44° to 0.002°, and γ varies from −3.52° to 0°. As expected, the biggest position error occurred along the x–y plane in $\{s\}$.

4.2 Shoulder Flexion–Extension Task

In this task, the same procedure is followed, except, the exoskeleton joint being actuated this time is J_3 instead of J_4, to generate the shoulder flexion–extension task. In the same manner, the coordinates of the human model were adjusted to produce this specific task. The derived position error in $\hat{x}$ varies from − 40.34 to 0 mm, $\hat{y}$ varies from − 40.95 to 0 mm, $\hat{z}$ varies from − 24.58 to 0.135 mm. Additionally, the orientation error in α varies from 0° to 6.61°, β varies from s − 0.79° to 3.57°, and γ varies from 0° to 0.33°. These errors are presented in Fig. 5. As shown, the position errors for this task are similar to the ones shown for the previous task. This was expected since both tasks are similar, but are performed within a different plane.

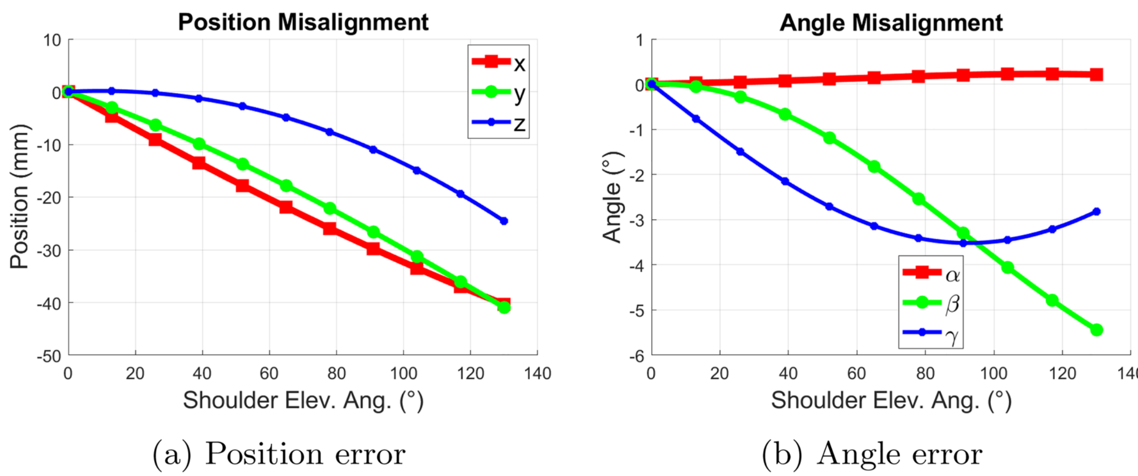

Fig. 4 Position and orientation errors for the shoulder abduction–adduction task

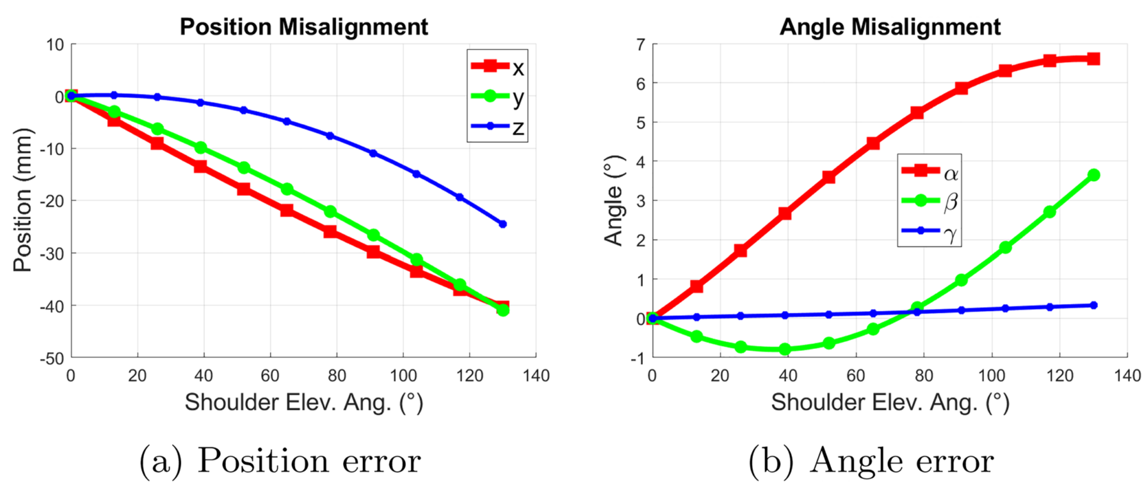

Fig. 5 Position and orientation errors for the shoulder flexion–extension task

4.3 Elbow Flexion–Extension Task

For the last task, the misalignment at the elbow joint is addressed. The simulation is proceeded as the previous tasks, but the J_4 exoskeleton joint coordinate is varied from 0° to 130° and vice-versa; the human model joint corresponding to the elbow is varied with the same range. All the other coordinates for the exoskeleton and the human model are set to 0° for the remaining of the task. The resultant errors for the position and the orientation for this task are shown in Fig. 6. The derived position errors are negligible in all directions, as seen in Fig. 6a. On the other hand, the orientation errors are not; they presented the following errors: α varies from -1.28° to 1.42°, β varies from 0° to 6.26°, and γ varies from 0° to 0.15°. These errors are shown in Fig. 6b.

4.4 Impairment Analysis of the Shoulder Joint

The impairment level found on the shoulder from the abduction–adduction and flexion–extension tasks are similar in terms of position, but different in orientation. Both cases showed that the maximum position impairment values are located in the sagittal plane of the human model; in our case, the $\hat{x} - \hat{y}$ plane.

To analyze the impairment caused by misalignment between the shoulder joint and the respective exoskeleton joint, the resultant maximum impairment values from the tasks 4.1 and 4.2 are gathered, which occur when the elevation angle on the shoulder is 130°. This is presented in Table 1. The values found in this study are coherent with the ones presented in [23], where a translation along the $\hat{y} - axis$ goes from 0 mm to around 100 mm when the shoulder elevation angle goes from 0° to 180°. These values are used to produce a new human model where the center of rotation of the shoulder joint has been translated and rotated using the values obtained.

Table 1 Maximum position and rotation values

x	y	z	α	β	γ
− 40.34 mm	− 40.95 mm	− 24.58 mm	0.2°	− 5.44°	− 2.81°

OpenSim has the ability to report the length of a muscle tendon within a model when given the kinematic information of its generalized coordinates. The muscle tendons are the connective tissues that attach the muscles to the bones. Therefore, any variation outside of the normal length could strain them. This would lead to an injury upon a healthy individual or cause severe pain to a patient undergoing rehabilitation. Therefore, misalignment will be assessed through the deformation of the muscle tendons due to impairment. Two muscle groups in the shoulder joint are targeted: the rotator cuff muscles and the deltoid muscle group, [24]. The former is composed of the supraspitnatus, infraspinatus, subscrapularis and teres minor; this group provides important structural support to the glenohumeral joint since it maintains the stability of the humeral head into the glenoid cavity. The latter is composed of three parts: the deltoid anterior, middle, and posterior, which superficially cover the shoulder. Depending on which fibers are activated, there will be rotation and adduction along the humerus.

Two simulations are performed for the shoulder abduction–adduction task, shown in 4.1, using the healthy human model and the model with the induced misalignment. The results of the muscle-tendon lengths' variations throughout the task are shown in Fig.7 and Fig.8.

A variation in length and pattern is shown in Fig. 8 for each of the muscles. For the most part, the deltoid muscle group did not present a noticeable difference in its patterns,

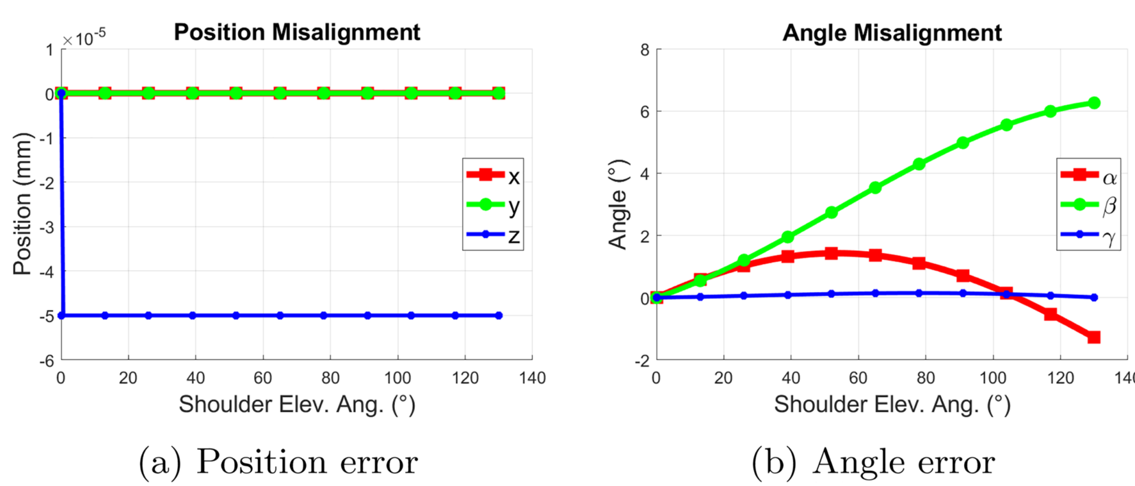

Fig. 6 Position and orientation errors for the elbow flexion–extension task

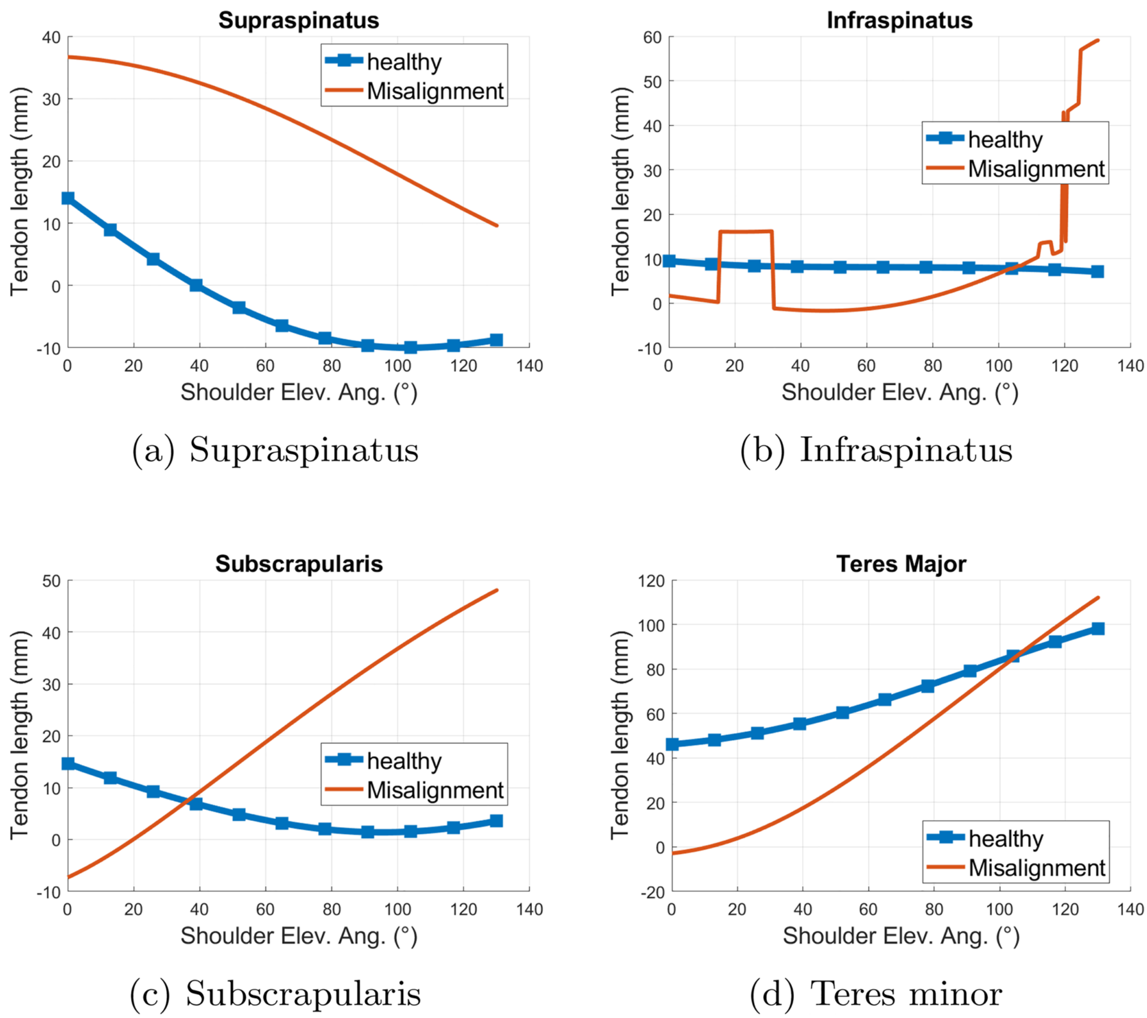

Fig. 7 Rotator cuff muscles

except for the deltoid posterior when the shoulder elevation angle varies from 45° to 130°, as shown in Fig. 8c. The change in tendon length for the deltoid anterior, middle and posterior are 65.7 mm, 65.91 mm and 27.82 mm, respectively. On the other hand, all the muscles composing the rotator cuff group demonstrated a change in pattern and an increase in length; the supraspinatus exhibited a maximum change of 33.9 mm, the infraspinatus exhibited a change of 52.02 mm, the subscapularis exhibited a change of 44.67 mm, and the teres minor exhibited a change of 56.21 mm. These changes in tendon lengths are likely to lead to discomfort and pain, especially upon individuals whose tendons are strained.

4.5 Impairment Analysis of the Elbow Joint

In the previous subsection, the impairment level of the shoulder was addressed, in this one, the elbow joint impairment will be investigated based on the results obtained during the elbow flexion–extension task, shown in Sect. 4.3. The position errors demonstrated negligible relative motion between the exoskeleton and human joints. However, orientation errors demonstrated a small level of misalignment, as shown in Fig. 6. The OpenSim model of the elbow is composed of nine muscles. The main flexor muscles are the biceps (long and short), the brachialis, and the brachioradialis. The main extensor muscles are the triceps (long, lateral, and medial) and the anconeus muscles. Finally, the prime supinator of the forearm is the supinator muscle [25].

The experiment procedure for this subsection is identical to the previous ones, except the joint being actuated is the elbow joint. The OpenSim model of the upper limb was offset at the elbow joint using the results of Sect. 4.3. Out of the nine muscles, only the anconeus muscle showed a small variation on its tendon length, which is presented in Fig. 9. This is a small muscle that attaches the lateral side of the humerus and the medial side of the ulna. This muscle is the main extensor contributor at low elbow-flexion angles [26].

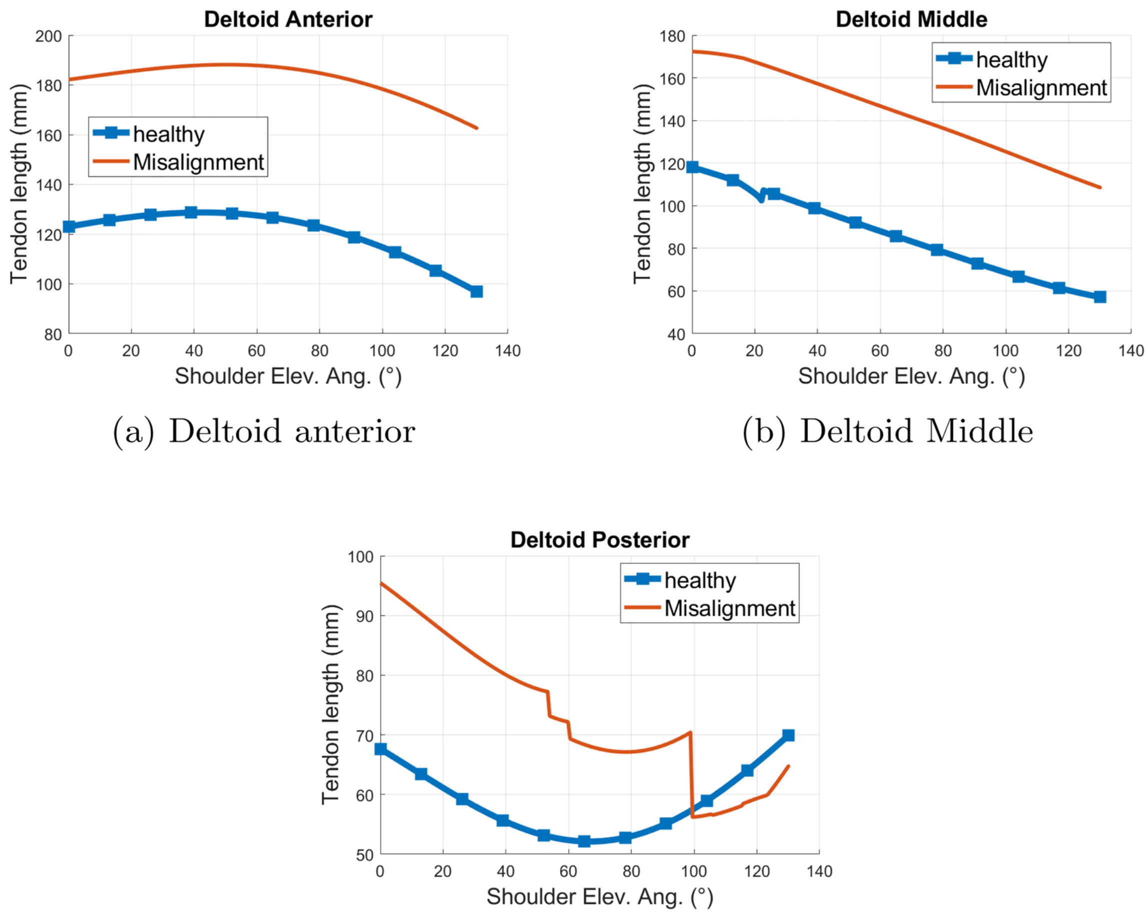

(a) Deltoid anterior

(b) Deltoid Middle

(c) Deltoid posterior

Fig. 8 Deltoid group of muscles

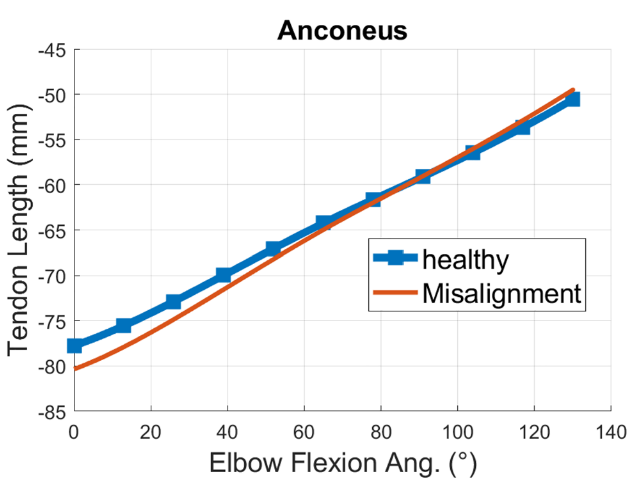

Fig. 9 Anconeus muscle

This fact explains why the highest change in tendon length occurred at low elbow-flexion angles, since the muscle is under more stressed. In addition, its size makes it susceptible to angle changes.

5 Conclusion

Through the proposed methodology, the variation on muscle tendons' lengths due to the discrepancies of human joints' positions and orientations with respect to their exoskeleton counterpart is quantified. Results showed that in the case of the shoulder, the maximum changes in muscle-tendon length due to a misalignment induced at the human model were shown at the deltoid anterior, middle and posterior muscles with 65.7 mm, 65.91 mm and 27.82 mm, respectively. Likewise, the supraspinatus exhibited a maximum change of 33.9 mm, the infraspinatus exhibited a change of 52.02 mm, the subscapularis exhibited a change of 44.67 mm, and the teres minor exhibited a change of 56.21 mm. These changes can result in discomfort and pain, especially to individuals who are injured and have strained muscles. In this study, the effect of fitting, manufacturing tolerances, and imperfections in the exoskeleton prototype were not considered. Future study will be done to include kinematic information extracted from the exoskeleton prototype- human interaction using a state-of-the-art motion capture system in the OpenSim simulation.

Funding This research was funded by National Science Foundation Grant No. 1915872. The content is solely the author's responsibility.

Data Availability Statement all data generated or analysed during this study are included in this published article. If you need more information, contact the corresponding author.

Declarations

Conflict of interest the authors declare that they have no competing interests.

References

1. Krichevets, A. N., Sirotkina, E., Yevsevicheva, I., & Zeldin, L. (1995). Computer games as a means of movement rehabilitation. *Disability and Rehabilitation, 17*(2), 100–105.
2. Meng, Q., Xiang, S., & Yu, H. (2017) Soft robotic hand exoskeleton systems: Review and challenges surrounding the technology. In: Proceedings of the 2nd International Conference on Electrical, Automation and Mechanical Engineering (EAME 2017), Shanghai, China; 2017. p. 23–24.
3. Lum, P. S., Burgar, C. G., Shor, P. C., Majmundar, M., & Van der Loos, M. (2002). Robot-assisted movement training compared with conventional therapy techniques for the rehabilitation of upper-limb motor function after stroke. *Archives of Physical Medicine and Rehabilitation, 83*(7), 952–959.
4. Staubli, P., Nef, T., Klamroth-Marganska, V., & Riener, R. (2009). Effects of intensive arm training with the rehabilitation robot ARMin II in chronic stroke patients: four single-cases. *Journal of Neuroengineering and Rehabilitation, 6*(1), 1–10.
5. Torricelli, D., Cortés, C., Lete, N., Bertelsen, Á., Gonzalez-Vargas, J. E., Del-Ama, A. J., et al. (2018). A subject-specific kinematic model to predict human motion in exoskeleton-assisted gait. *Frontiers in Neurorobotics, 12,* 18.
6. Delgado, P., Alekhya, S., Majidirad, A., Hakansson, N. A., Desai, J., & Yihun, Y. (2020). Shoulder kinematics assessment towards exoskeleton development. *Applied Sciences, 10*(18), 6336.
7. Niu, Y., Song, Z., & Dai, J. (2018). Kinematic analysis and optimization of a planar parallel compliant mechanism for self-alignment knee exoskeleton. *Mechanical Sciences, 9*(2), 405–416.
8. Zanotto, D., Akiyama, Y., Stegall, P., & Agrawal, S. K. (2015). Knee joint misalignment in exoskeletons for the lower extremities: Effects on user's gait. *IEEE Transactions on Robotics, 31*(4), 978–987.
9. Heidari, O., Wolbrecht, E. T., Perez-Gracia, A., & Yihun, Y. S. (2018). A task-based design methodology for robotic exoskeletons. *Journal of Rehabilitation and Assistive Technologies Engineering, 5,* 2055668318800672.
10. Aguirre-Ollinger, G., Colgate, J. E., Peshkin, M. A., & Goswami, A. (2011). Design of an active one-degree-of-freedom lower-limb exoskeleton with inertia compensation. *The International Journal of Robotics Research, 30*(4), 486–499.
11. Puzi, A.A., Sidek, S., & Sado, F. (2017). Mechanical impedance modeling of human arm: A survey. In: IOP Conference Series: Materials Science and Engineering. vol. 184. IOP Publishing; 2017. p. 012041.
12. Hefzy, M. S., & Abdel-Rahman, E. M. (2019). Three-dimensional dynamic anatomical modeling of the human knee joint. *Musculoskeletal Models and Techniques* (pp. 1–1). New York: CRC Press.
13. Zeiaee, A., Soltani-Zarrin, R., Langari, R., & Tafreshi, R. (2017). Design and kinematic analysis of a novel upper limb exoskeleton for rehabilitation of stroke patients. In: 2017 International Conference on Rehabilitation Robotics (ICORR). IEEE;p. 759–764.
14. Sposito, M., Di Natali, C., Toxiri, S., Caldwell, D. G., De Momi, E., & Ortiz, J. (2020). Exoskeleton kinematic design robustness: An assessment method to account for human variability. *Wearable Technologies, 1*.
15. de Kruif, B. J., Schmidhauser, E., Stadler, K. S., & O'Sullivan, L. W. (2017). Simulation architecture for modelling interaction between user and elbow-articulated exoskeleton. *Journal of Bionic Engineering, 14*(4), 706–715.
16. Li, N., Yang, T., Yang, Y., Yu, P., Xue, X., Zhao, X., et al. (2020). Bioinspired musculoskeletal model-based soft wrist exoskeleton for stroke rehabilitation. *Journal of Bionic Engineering, 17*(6), 1163–1174.
17. Ballen-Moreno, F., Bautista, M., Provot, T., Bourgain, M., Cifuentes, C. A., & Múnera, M. (2022). Development of a 3D relative motion method for human-robot interaction assessment. *Sensors, 22*(6), 2411.
18. Graichen, H., Stammberger, T., Bonel, H., Englmeier, K. H., Reiser, M., & Eckstein, F. (2000). Glenohumeral translation during active and passive elevation of the shoulder-a 3D open-MRI study. *Journal of Biomechanics, 33*(5), 609–613.
19. Lee, B., Lee, S. C., & Han, Cs. (2020). Design of fixations for an exoskeleton device with joint axis misalignments. *International Journal of Precision Engineering and Manufacturing, 21*(7), 1291–1298.
20. Delp, S. L., Anderson, F. C., Arnold, A. S., Loan, P., Habib, A., John, C. T., et al. (2007). OpenSim: Open-source software to create and analyze dynamic simulations of movement. *IEEE Transactions on Biomedical Engineering, 54*(11), 1940–1950.
21. Holzbaur, K. R., Murray, W. M., & Delp, S. L. (2005). A model of the upper extremity for simulating musculoskeletal surgery and analyzing neuromuscular control. *Annals of Biomedical Engineering, 33*(6), 829–840.
22. Saul, K. R., Hu, X., Goehler, C. M., Vidt, M. E., Daly, M., Velisar, A., et al. (2015). Benchmarking of dynamic simulation predictions in two software platforms using an upper limb musculoskeletal model. *Computer Methods in Biomechanics and Biomedical Engineering, 18*(13), 1445–1458.
23. Nef, T., Guidali, M., & Riener, R. (2009). ARMin III-arm therapy exoskeleton with an ergonomic shoulder actuation. *Applied Bionics and Biomechanics, 6*(2), 127–142.
24. Eovaldi, B. J., & Varacallo, M. (2018). *Anatomy, shoulder and upper limb, shoulder muscles*. StatPearls Treasure Island: StatPearls.
25. Wilk, K. E., Arrigo, C., Yenchak, A. J., & Andrews, J. R. (2012). 13—Rehabilitation of Elbow Injuries. In J. R. Andrews, G. L. Harrelson, & K. E. Wilk (Eds.), *Physical Rehabilitation of the Injured Athlete* (4th ed., pp. 232–258). Philadelphia: W.B. Saunders.
26. Pereira, B. P. (2013). Revisiting the anatomy and biomechanics of the anconeus muscle and its role in elbow stability. *Annals of Anatomy-Anatomischer Anzeiger, 195*(4), 365–370.